Compumag 2011

12 - 15 July 2011, Sydney, Australia

18th International Conference on the Computation of Electromagnetic Fields

(www.compumag2011.com)

TECHNICAL PROGRAM

(Draft on 22 June 2011)

PA3.9 (ID 144)
Magnetic Equivalent Circuit for Saturation Modeling of a Deep-bar Induction Motor
Huynh, Van Khang; Hellman, Hannu-Pekka; Arkkio, Antero
Aalto University, Finland

PA3.10 (ID 149)
Core Loss Modeling for Permanent Magnet Motor Based on Flux Variation Locus and Finite Element Method
Huang, Yunkai (1); Dong, Jianning (1); Lin, Heyun (1); Guo, Youguang (2); Zhu, Jianguo (2)
1: School of Electrical Engineering, Southeast University, Nanjing, China; 2: School of Electrical, Mechanical and Mechatronic Systems, University of Technology Sydney, Australia

PA3.11 (ID 156)
Magnetic Field in a Transverse- and Axial-flux Permanent-Magnet Synchronous Generator from 3-D FEA
Chan, Tze-Fun (1); Wang, Weimin (1); Lai, Loi Lei (2)
1: The Hong Kong Polytechnic University, China, Peoples Republic of; 2: City University London, UK

PA3.12 (ID 158)
Mechanical Stress Reduction of Rotor Core of Interior Permanent Magnet Synchronous Motor
Jung, Jae-Woo (1); Hong, Jung-Pyo (1); Jeon, Seong-Min (2)
1: Hanyang University, Korea, South (Republic of); 2: S&T Daewoo, Korea, South (Republic of)

PA3.13 (ID 159)
Modeling of Switched Reluctance Motor for Inter-Turn Winding Short-Circuit Fault
Chen, Hao (1); Lu, Shengli (1); Chen, Zhe (2)
1: China University of Mining & Technology, China, Peoples Republic of; 2: Institute of Energy Technology, Aalborg University, Aalborg 9220, Denmark

PA3.14 (ID 165)
A Dynamic Cosimulation Approach for a Switched Reluctance Starter/Generator Using Maxwell SPICE and Simplorer
Ding, Wen
Xi'an jiaotong University, China, Peoples Republic of

PA3.15 (ID 173)
The Analysis of a Novel Transverse-flux Linear Oscillating Actuator
Lu, Qinfen; Yu, Minghu; Ye, Yunyue; Fang, Youtong
Zhejiang University, China, Peoples Republic of

PA3.16 (ID 222)
Conductive EMI Noise Analysis for Switched Reluctance Motor Drive
Chen, Hao; Zhao, Y; Qiu, X
China University of Mining & Technology, China, Peoples Republic of

PA3.17 (ID 175)
Analytical Calculation of Flux-Linkage Characteristics of Switched Reluctance Linear Generator
Chen, Hao; Lu, S; Zhou, X; Sun, C
China University of Mining & Technology, China, Peoples Republic o

Mechanical Stress Reduction of Rotor Core of Interior Permanent Magnet Synchronous Motor

Jae-Woo Jung[1], Byeong-Hwa Lee[1], Do-Jin Kim[1], Jung-Pyo Hong[1], *Senior Member, IEEE*, Jae-Young Kim[2], and Seong-Min Jeon[2]

[1]Department of Automotive Engineering, Hanyang University, Seoul, Korea
[2]Motor R&D Center, S&T Daewoo Co., Ltd., Busan, Korea

In this paper, the bridge shape of interior permanent magnet synchronous motor (IPMSM) is designed for integrated starter and generator (ISG) which is applied in hybrid electric vehicle (HEV). Mechanical stress of rotor core which is caused by centrifugal force is the main issue when IPMSM is operated at high speed. The bridge is thin area in rotor core where is mechanically weak point and the shape of bridge significantly affects leakage flux and electromagnetic performance. Therefore, bridge should be designed considering both mechanic and electromagnetic characteristics. In the design process, we firstly find a shape of bridge has low leakage flux and mechanical stress. Next, the calculation of mechanical stress and the electromagnetic characteristics are performed by finite element analysis (FEA). The mechanical stress in rotor core is not maximized in steady high speed but dynamical high momentum. Therefore, transient FEA is necessary to consider the dynamic speed changing in real speed profile for durability experiment. Before the verification test, fatigue characteristic is investigated by using S-N curve of rotor core material. Lastly, the burst test of rotor is performed and the deformation of rotor core is compared between prototype and designed model to verify the design method.

***Index Terms*— Bridge, Burst test, Centrifugal force, Fatigue, IPMSM, Mechanical stress, Mechanical transient FEA, S-N curve**

I. Introduction

ACCORDING TO the development of the electric motor for automotive applications especially for the electric vehicle and the hybrid electric vehicle, high speed electric motor has been researched by many experts. Generally, motor volume is determined by the maximum torque and the cooling condition. Therefore, increasing the speed of motor is the effective design strategy for reducing a total size of motor with the output same power [1].

Interior permanent magnet synchronous motor (IPMSM) is one of the attractive solutions for the high speed electric machine because it has high torque and wide speed range by mean of current vector control [2]. However, there is mechanically weak location in rotor at high speed operation because centrifugal force is concentrated locally in the bridge which is relatively thin area in rotor core. The bridge of rotor core hugely affects magnetic characteristics because it mainly determines leakage flux [3]. Thinner bridge will result in better electromagnetic performance due to less leakage flux, but it may not be strong enough to withstand the centrifugal forces at high speed [4]. Therefore, it is important to design the shape of bridge considering such aspects.

In this paper, to reduce mechanical stress of rotor core, IPMSM is designed with analysis of magnetic characteristics as well as mechanical analysis using finite element analysis (FEA). Mechanical stress is not maximized at steady high speed but at high momentum. Therefore, transient FEA is applied to calculate mechanical stress considering the acceleration and deceleration of rotor core. In this simulation, Von Mises stress is applied. Before the verification test, fatigue characteristic is investigated by using S-N curve from the test of the rotor core material sample.

The entire design process is shown below:

1. A study on the root-cause analysis of mechanical problem of prototype.
2. Selection of candidate model.
3. Analysis of magnetic field and centrifugal force. (Steady static condition)
4. Mechanical transient analysis and electromagnetic field analysis.
5. Investigation of fatigue characteristic using S-N curve. (S-N curve is derived from the material test data)
6. Experimental verification of the final design model. (Rotor burst test)

II. Root-Cause analysis of mechanical problem

The centrifugal force is proportional to square of rotating speed as shown in equation (1).

$$F = \frac{mv^2}{r}. \tag{1}$$

where F is centrifugal force, m is mass, v is rotating velocity and r is radius of mass. Centrifugal force is proportional to square of velocity. Therefore, it is necessary to calculate the mechanical stress caused by centrifugal force at high speed.

Fig. 1 shows the bridge shape of prototype which has been designed with relatively longer than ordinary model because such structure was designed based on optimization of noise reduction [5]. Unfortunately, long bridge structure for noise reduction increases mechanical stress locally. Fig. 1 shows rotor lamination and the segment of rotor core which burst under the high centrifugal force during high speed operation. Once a rotor bursts, chips scratch off the end-turn and finally the motor would be severely damaged.

Manuscript received July 1, 2011 (date on which paper was submitted for review). Manuscript received July 7, 2011.
Corresponding author: Jung-Pyo Hong (e-mail: hongjp@hanyang.ac.kr).
Digital Object Identifier inserted by IEEE

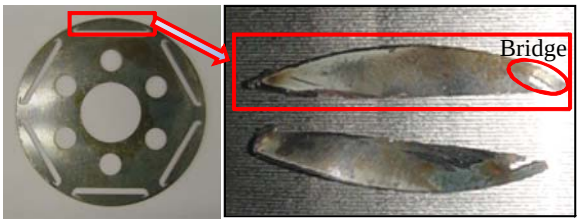

(a) Rotor core lamination (b) Segment of rotor core
Fig. 1. Burst rotor core of prototype.

III. Mechanical and Electromagnetic Analysis

A. Condition of mechanical computation

In IPMSM, permanent magnets (PM) are buried inside of rotor core to employ a hybrid torque generation [6]. In order to insert the PM into rotor core, it should have dimensional tolerance between PM and rotor core. Generally, the space caused by this tolerance is filled with industrial adhesive to increase strength and solidity between PM and the core. However, bonding strength becomes weaker as time passes and this strength is not permanently constant.

Fig. 2 shows the calculation result of mechanical stress of bonded and non-bonded motor where the core material properties are shown in Table I. Analysis model shown in Fig. 2 (a) is the ideal case of assembly because both top and bottom side of PM are bonded to rotor core. Mechanical stress is distributed in large area of rotor core and PM. Therefore, maximum value of mechanical stress is significantly low. On the other hand, maximum mechanical stress of Non-bonded model (b) is much higher than Bonded model (a) because Non-bonded model (b) does not have bonding strength of adhesive between PM and rotor core. In Non-bonded model, only top surface of PM is attached to the rotor core due to centrifugal force and it adds to stress on the corner of bridge. Nevertheless, even if adhesive is applied, it is more practical to consider this as Non-bonded model in durability perspective as adhesive effect becomes weaker. Therefore, effect of adhesive on PM is ignored in the computation of mechanical stress.

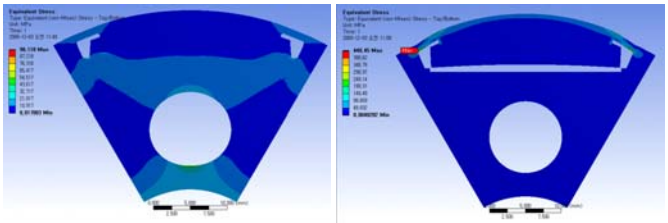

(a) Bonded model (b) Non-bonded model
Fig. 2. Equivalent stress with respect to existence of adhesive

TABLE I
Material Properties of Rotor Core

Quantity	Unit	Value
Density	kg/m^3	7600
Young's modulus	GPa	207
Poisson's ratio	-	0.31
Tensile strength	Mpa	550
Yield strength	Mpa	390

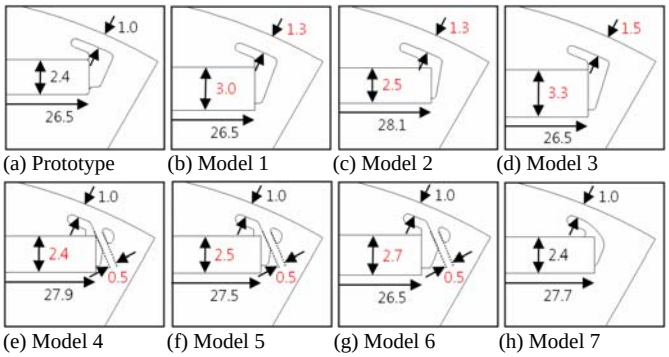

(a) Prototype (b) Model 1 (c) Model 2 (d) Model 3
(e) Model 4 (f) Model 5 (g) Model 6 (h) Model 7
Fig. 3. Bridge shape of prototype and candidate models

TABLE II
Characteristics of Prototype and Candidate Model

Model	Mechanical stress [Mpa]	Bemf_L-L [Vrms]	Torque [Nm]	PM Volume [mm^3]
Prototype	437.0	23.3	45.9	5088.0
Model 1	400.2	22.9	46.6	6360.0
Model 2	354.7	23.3	45.0	5620.0
Model 3	390.0	23.3	46.4	6996.0
Model 4	371.1	23.3	45.2	5356.8
Model 5	364.2	23.4	45.6	5500.0
Model 6	389.9	23.0	46.3	5724.0
Model 7	231.8	23.2	45.9	5318.4

Bemf_L-L: Fundamental RMS value of Line to line back EMF. (FEA result)
Torque: Calculated by FEA under the maximum value of input current.
PM Volume: Volume of permanent magnet per single pole.

B. Analysis of candidate models

There are many design methods to increase the stiffness of rotor core. For example, drilling holes around the bridge and H- or I-bar bridge are commonly used [7]-[9]. In this paper, increasing the bridge thickness, dual bridge type, and round corner bridge type are investigated as shown in Fig.3.

Shapes of Model 1 to 3 are almost the same with prototype except the thickness of bridge. Models 4 to 6 are dual bridge types and mechanical stress can be distributed to these two bridges. The bridge shape of Model 7 is almost the same with prototype except the corner shape of bridge. Change in bridge shape is one of the driving factors of increasing leakage flux. Therefore, the shape of PM of all models is redesigned to have the back-EMF almost the same as the prototype one. After redesigning the PM, PM volume of all candidate models has been increased. Table I. shows magnetic characteristics, PM volume and centrifugal force of each model. The assumptions and conditions employed in this calculation are shown as follows [9].

- Steady-state speed conditions only (Maximum speed);
- Temperature effects neglected;
- Yield indicated by planar Von Mises stress;
- Forces of electromagnetic origin considered negligible;
- Vibration and rotor shaft dynamical forces neglected.

Design methods of increasing the thickness of bridge is excluded in selection of final design model because decreasing rate of mechanical stress against increasing rate the PM volume is relatively low. Meanwhile, dual bridge type is appropriate method in the 'research level' but it is not suitable for mass production due to durability of dies. Moreover, the

thickness of dual bridge is too thin. Round shape bridge model, Model 7, has the lowest increasing rate of PM volume and mechanical stress. Therefore, Model 7 is selected as final design model.

C. *Theory of mechanical transient analysis*

The transient dynamic equilibrium equation of interest is as follows for a linear structure.

$$[M]\{\ddot{u}\}+[C]\{\dot{u}\}+[K]\{u\}=\{F^a\} \quad (2)$$

where [M] is structural mass matrix, [C] is structural damping matrix, [K] is structural stiffness matrix, $\{\ddot{u}\}$ is nodal acceleration vector, $\{\dot{u}\}$ is nodal velocity vector, $\{u\}$ is nodal displacement vector and $\{F^a\}$ is applied load vector.
In this paper, the Newmark method uses finite difference expansions in the time interval Δt.

$$\{u_{n+1}\}=\{\dot{u}_n\}+[(1-\delta)\{\ddot{u}_n\}+\delta\{\ddot{u}_{n+1}\}]\Delta t \quad (3)$$

$$\{u_{n+1}\}=\{u_n\}+\{\dot{u}_n\}\Delta t+\left[(1/2-\alpha)\{\ddot{u}_n\}+\alpha\{\ddot{u}_{n+1}\}\right]\Delta t^2 \quad (4)$$

where α and δ are Newmark integration parameters. Since the primary aim is the computation of displacements $\{u_{n+1}\}$, the governing equation (2) is evaluated at time $\{t_{n+1}\}$ as bellow.

$$[M]\{\ddot{u}_{n+1}\}+[C]\{\dot{u}_{n+1}\}+[K]\{u_{n+1}\}=\{F^a\} \quad (5)$$

The solution for the displacement at time $\{t_{n+1}\}$ is obtained by first rearranging equation (3) and (4) [10].

D. *Result of mechanical transient analysis*

Generally, most of study for improvement of stiffness of rotor core in IPMSM is considered only at maximum operating speed, without any dynamical momentum interpretation. However, centrifugal force is maximized when the rotor is rotating with high angular momentum, not the constant speed. In this paper, IPMSM is applied to Integrated Starter and Generator (ISG) of which operating speed is dynamically changed as real driving condition. Therefore, mechanical transient analysis for calculating of mechanical stress is required to consider such an operating condition.

Mechanical transient analysis is performed both Prototype and the final design model, Model 7. Commercial software 'ANSYS Workbench' is employed to calculate centrifugal force and mechanical stress on both models. Fig. 4 shows boundary condition of mechanical transient analysis. Three boundary conditions are employed as shown on following:

- A-Point : Transient Rotation Velocity
- B-Point : Frictionless Support (Symmetric condition)
- C-Point : Fixed support

Speed profile shown in Fig. 5 is applied to simulation condition A-point. The speed profile is a part of durability test condition of ISG. The original test condition is more complicated than Fig. 5. It has been simplified for FEA considering the computation time efficiency.

FEA results of both models are shown in Fig. 6. The tendency of mechanical stress versus time is similar to the graph for speed versus time. The maximum value of centrifugal force occurs at 1577.1 [sec] due to maximum momentum of rotor at this point. Fig. 7 shows calculated mechanical stress distribution. In case of prototype, mechanical stress is concentrated on the corner of bridge and maximum value is 465Mpa which is different from the calculated value at steady state condition shown in Table II. On the other hand, mechanical stress of final design model is distributed relatively large area around the corner of bridge. Maximum value 240Mpa is also higher than the calculated result shown in Table II.

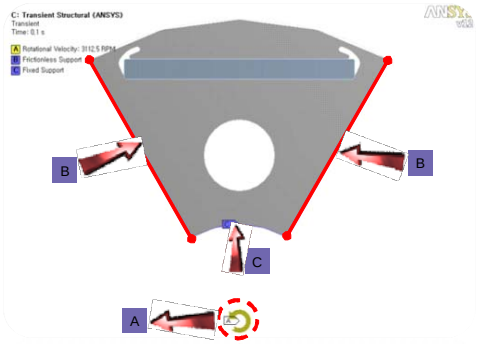

Fig. 4. Boundary conditions

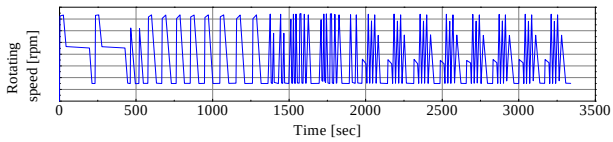

Fig. 5. Durability test profile of ISG (Time versus Rotating speed)

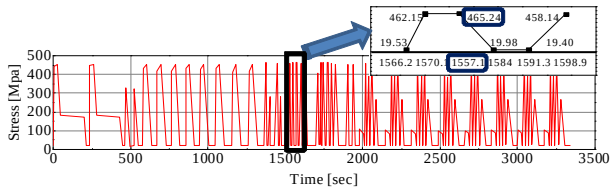

(a) Prototype

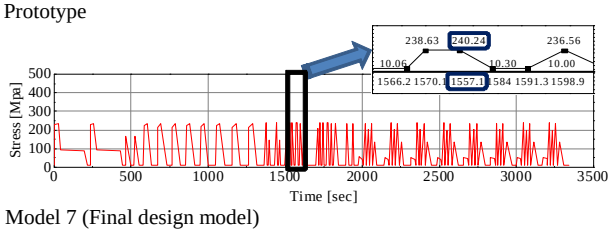

(b) Model 7 (Final design model)

Fig. 6. Result of transient analysis (Time versus Mechanical stress)

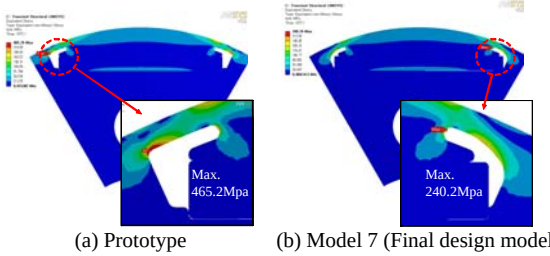

(a) Prototype (b) Model 7 (Final design model)

Fig. 7. Distribution of mechanical stress

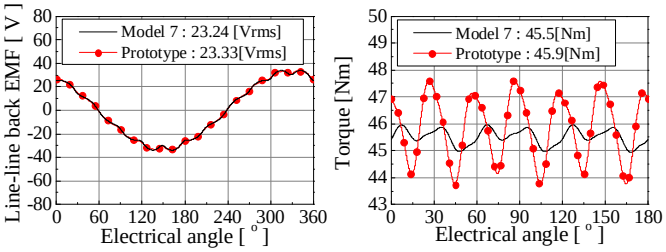

(a) Line to line Back EMF (b) Torque waveforms

Fig. 8. Result of electromagnetic characteristics

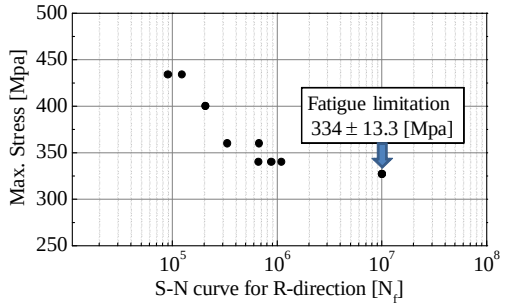

Fig. 9. S-N curve

E. *Electromagnetic characteristics*

Electromagnetic analysis is performed as shown in Table II. The graph of back-EMF and torque ripple waveforms are shown in Fig. 8. The R.M.S. fundamental values of back EMF of both models are almost the same. Average torque values of both models are also similar with each other. This means that the characteristics curves of both motors are almost the same. Fortunately, torque ripple of Final design model (Model 7) is much lower than prototype, which implies that noise can be improved by design of mechanical stress reduction [5].

IV. Test for Verification

A. *Fatigue characteristic*

Even though maximum stress in bridge is lower than yield strength of core material, rotor core could be broken as time passes due to fatigue characteristics of material. Therefore maximum stress of bridge should be lower than fatigue limitation. In this time, S-N curve is employed to verify fatigue characteristics of material. Fig. 9 shows experimental data of S-N curve of rotor core. The fatigue limitation is 334±13.3[Mpa] and this value is higher than maximum stress of designed model 240.2[Mpa]. Therefore, stiffness of designed model guarantees against fatigue failure.

B. *Rotor burst test*

In order to verify the design method, rotor burst test has been conducted. It is hardly possible to measure the stress in the bridge during rotor rotating situation. Therefore, measurement of stress is substituted for measuring the deformation. The deformation is measured by Vernier calipers after rotor rotating at a certain speed. The measured result of deformation versus rotating speed is shown in Fig. 10. Deformation value at 33,000rpm of designed model is approximately 35% lower than the value of prototype.

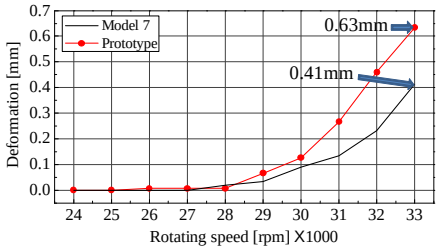

Fig. 10. The result of rotor burst test

V. Conclusion

Mechanical stress in the rotor core of IPMSM is one of the main design factors in the high speed application. In general, centrifugal force and mechanical stress are calculated by FEA with condition of constant speed. However, this calculation method has limitation when the motor is operated with rapid change in speed. Therefore, mechanical transient analysis is necessary to consider the variable speed operating condition.

This paper introduces FEA simulation as well as design of rotor core to reduce mechanical stress in the core bridge. Moreover, S-N curve of rotor core material as an experimental result has been presented to guarantee the validity of model against fatigue failure. The experimental verification also has been conducted by measuring the deformation of rotor core versus rotor rotating speed.

Overall, the design method in this paper would be helpful to the design of IPMSM with high speed applications.

References

[1] Pickup I.E.D., Tipping D., Hesmondhalgh D.E., AI Zahawi B.A.T., “A 250,000rpm drilling spindle using a permanent magnet motor,” Proc.ICEM’96, Vigo, Spain, 337-342, 1996.

[2] Shigeo Morimoto, Yoji Takeda, Takao Hirasa, and Katsunori Taniguchi, “Expansion of Operating Limits for Permanent Magnet Motor by Current Vector Control Considering Inverter Capacity,” *IEEE Trans. Ind. Appl.*, vol. 26, no. 5, pp. 866-871, Sep./Oct. 1990.

[3] G. X. Zhou, R. Y. Tang, D. H. Lee, and J. W. Ahn, “Field circuit coupling optimization design of the main electromagnetic parameters of permanent magnet synchronous motor,” *KIEE, J. Electr. Eng. Technol.*, vol. 3, no. 1, pp. 88–93, 2008.

[4] K. H. Ha, J. P. Hong, G. T. Kim, Y.H. Choi, W. J. Chung, “Mechanical Vibration and Stress Analysis of the Link of Interior Permanent Magnet type Synchronous Motor,” Electric Machines and Drives, 1999, *IEMD* ‘99

[5] Jae-Woo Jung, Sang-Ho Lee, Geun-Ho Lee, Jung-Pyo Hong, Dong-Hoon Lee, and Ki-Nam Kim, “Reduction Design of Vibration and Noise in IPMSM type Integrated Starter and Generator for HEV,” *IEEE Trans. Magn.*, vol. 46, no. 6, pp. 2454-2457, Jun. 2010.

[6] Liang Fang, Jae-Woo Jung, Jung-Pyo Hong, and Jung-Ho Lee, “Study on High-Efficiency Performance in Interior Permanent Magnet Synchronous Motor With Double-Layer PM Design,” *IEEE Trans. Magn.*, vol. 44, no. 11, pp. 4393-4396, Nov. 2008.

[7] Tae-geun Lee, Do-Jin Kim, Jung-Pyo Hong, “Performance Improvement by Making Holes of Interior Permanent Magnet Synchronous Motor,” IEEE ICEMS 2009.

[8] Zeyin Han, Haodong Yang, and Yangsheng Chen, “Investigation of the Rotor Mechanical Stresses of Various Interior Permanent Magnet Motors,” NSFC

[9] E.C. Lovelace, T.M. Jahns, T.A. Keim, and J.H. Lang, “Mechanical design considerations for conventionally laminated, high speed, interior PM synchronous machine rotors,” *IEEE Trans. Ind. Appl.*, vol. 40, no. 3, pp. 806-812, May/June 2004.

[10] K. J. Bathe, “Finite Element Procedures,” Prentice-Hall, Englewood Cliffs, 1996.